Journal of the European Ceramic Society **17** (1997) 1309–1315
© 1997 Elsevier Science Limited
Printed in Great Britain. All rights reserved
PII: S0955-2219(96)00241-5
0955-2219/97/$17.00

Kinetics and Phase Evolution During Carbothermal Synthesis of Titanium Carbide from Carbon-Coated Titania Powder

Rasit Koc

Department of Mechanical Engineering and Energy Processes, Southern Illinois University at Carbondale, Carbondale, IL 62901, USA

(Received 13 September 1996; revised version received 7 November 1996; accepted 11 November 1996)

Abstract

Kinetics and phase evolution of the TiC formation process by carbothermal reduction of carbon-coated titania (TiO_2) powder were investigated using TGA, XRD, and chemical analysis. The TiC synthesis in the present work proceeded via forming titanium oxycarbide (TiC_xO_y) followed by its purification toward titanium carbide (TiC). The formation of TiC_xO_y was achieved via two routes. The uniformly coated pyrolytic carbon on fine titania particles formed the first TiC_xO_y phase at temperature of 1000°C. The additional TiC_xO_y formed from Ti_3O_5 as temperature increased. The activation energy of the additional TiC_xO_y formation process was calculated to be 278·1 kJ/mole. The resultant TiC powders prepared at 1550°C for 4 h in flowing argon showed fine particle size (0·1–0·3 μm), oxygen content of 0·57 wt%, lattice parameter of 4·331 Å, uniform particle shape, and loose agglomeration between particles. © *1997 Elsevier Science Limited.*

1 Introduction

Hard metals based on titanium carbide are finding increasing application as materials comparable in quality to the conventional hard-metal grades containing the strategic metal tungsten.[1] For advanced applications, titanium carbide powders with a homogeneous chemical composition, fine particle size, a narrow particle size distribution, and a loose agglomeration are required. Methods that have been developed to synthesize TiC powders include the direct carbonization of titanium metal (combustion synthesis)[2] or titanium hydride,[3] the gaseous pyrolysis of titanium halide such as $TiCl_4$ in a carbon-containing atmosphere,[4] and the carbothermal reduction of TiO_2 with carbon in controlled atmospheres at high temperatures.[5–7] Metallic titanium as a starting material is relatively expensive and, furthermore, the oxygen contained in the metal can hardly be reduced, so that the product is generally characterized by a high oxygen content.[5] Titanium chloride as a precursor is of importance in the field of chemical vapor deposition, but it is very expensive.

An inexpensive method of producing titanium carbide that has been applied commercially[6] involves the carbothermal reaction between titania (TiO_2) and carbon particles:

$$TiO_2(s) + 3\ C(s) = TiC(s) + 2\ CO(g) \qquad (1)$$

The actual TiC production by the carbothermal process is achieved at much higher temperatures than the thermodynamic onset temperature of reaction (1) (1289°C when partial pressure of CO gas is 1 atm.[8]) because of kinetic barriers such as limited contact area between reactants and uneven distribution of carbon in the reactants. These limitations and higher temperature processing result in grain growth, particle coalescence, non-uniform particle shape, considerable quantities of unreacted TiO_2 and carbon in the final product. For example, in the commercial production of TiC,[6] reactants are fired at 1900–2300°C in an inert atmosphere when sintered lumps of titanium carbide form. These then require crushing using jaw crushers, and fine-milling thereafter.

The process presented in this work avoids the expense of the first two methods while surmounting the inability of the third (carbothermal reduction of TiO_2) to make a suitable product. It minimizes kinetic barriers by improving the way that carbon is introduced to the reactants. The process consists of two steps.[9] The first step is the coating of TiO_2 powders with carbon by decomposing a hydrocarbon gas (C_3H_6) at temperatures of 400–600°C. The second stage involves the

formation of TiC powders by promoting the carbothermal reduction of the carbon-coated TiO_2 particles in an inert atmosphere at temperatures of 1200–1550°C. This way of increasing contact area between reactants (reduction of kinetic barrier) should result in a more complete reaction and a purer product at a temperature closer to the thermodynamic onset point. The complete separation of the TiO_2 particles by coated carbon and the low-temperature processing should result in products with less particle agglomeration and uniform shape. In the present paper, the effectiveness of the carbon coating by the pyrolysis of propylene (C_3H_6), kinetics and phase evolution of the carbon-coated TiO_2 precursor in the subsequent firing conditions, and the characteristics of the resultant TiC powders are reported.

2 Experimental Procedure

As a preliminary step, the formation of the condensed phase of carbon by the pyrolysis of C_3H_6 was studied by obtaining equilibrium composition with one mole of C_3H_6 gas using a computer software (HSC Chemistry, Outokumpu Oy, Pori, Finland) based on a Gibbs free energy minimization routine. Figure 1 shows the equilibrium composition of major products from 1 mole of C_3H_6 gas at 2·72 atm (40 psi) pressure. This pressure ensured an efficient carbon deposition on TiO_2 surfaces (instead of forming individual carbon particles) so that the specific surface area of the precursor decreased from 60 m^2/g (as-received TiO_2 powders) to 44 m^2/g (after coating). As shown in Fig. 1, the reaction:

$$2\ C_3H_6(g) = 3\ C(s) + 3\ CH_4(g) \qquad (2)$$

is dominant at low temperatures while the formation of a high-purity condensed phase of carbon is

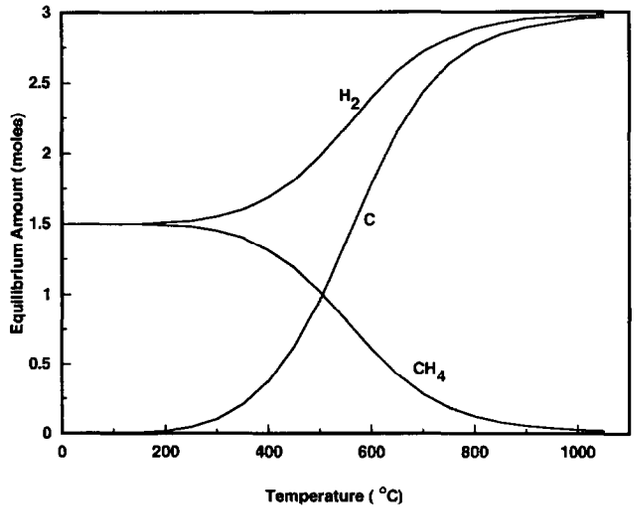

Fig. 1. Equilibrium composition of one mole of C_3H_6 gas with one mole of argon at various temperatures and 2·72 atm pressure.

accelerated at high temperatures according to the reaction:

$$C_3H_6(g) = 3\ C(s) + 3\ H_2(g) \qquad (3)$$

Based on Fig. 1, the pyrolysis temperature of hydrocarbon (C_3H_6) gas was determined to be 550°C for the carbon-coating step.

A rotating coating apparatus, consisting of a 10 cm ID × 35 cm long stainless steel vessel was used for preparing the carbon-coated titania precursor. About 20 g of titania powder (P-25, Degussa Corp., Ridgefield, NJ) was placed in the vessel followed by evacuation to a moderate vacuum level using a rotary vacuum pump. Then the propylene (C_3H_6) gas was filled into the vessel until pressure reached 2·72 atm. The vessel was then heated to 550°C while it was rotating. Thermal cracking of propylene increased the internal vessel pressure upon initiation of the carbon coating. The coating step was continued until about 32·6 wt% carbon was deposited, which required about 18 cycles (each cycle was 20 min). The weight percentage of the carbon in the precursor was based upon weight loss after firing at 650°C for 4 h in air.

For isothermal thermogravimetric analysis (TGA) (Model TG-17 l, Cahn Instruments, Inc., Cerritos, CA), 0·2 g of the carbon-coated titania precursor was taken in a cylindrical graphite holder (ID of 1·25 cm and height of 1·9 cm). The graphite holder was then placed in a cylindrical alumina holder (ID of 1·9 cm and height of 2·5 cm) with a platinum hanger. The sample (sample, graphite holder, and alumina holder) was hung on a high precision balance. The B-type thermocouple, protected by an alumina protecting tube, was placed at approximately 1 cm below the alumina sample holder. The system was enclosed by a perpendicularly positioned alumina tube furnace (ID of 3·2 cm). Argon gas was passed from bottom to top for 6 h before increasing temperature and continued throughout the run. In order to minimize the degree of reaction before reaching the final temperature, the maximum allowable heating rate of the instrument was applied for operation: 70°C/min up to 1000°C and then 20°C/min above 1000°C. After reaching the desired temperature (900–1400°C), the sample was fired for 2 h followed by furnace cooling down to 1000°C (at 10°C/min rate) where the furnace power was off. Data acquisition was performed every 5 s to a computer disk.

The samples fired in the TGA instrument at various temperatures were cooled down to room temperature and then were subjected to X-ray diffraction (XRD) (Model DMAX-B, Rigaku Corp., Tokyo, Japan) analyses for the study of phase evolution using Cu-K_α radiation and a zero-

background sample cell. Scanning angle was from 27 to 80° at 2°/min scanning speed.

For the production of TiC powders, 20 g of the carbon/titania mixture (~33 wt% carbon) was placed in a graphite boat and then the boat with sample was positioned in the center of a horizontally positioned alumina tube furnace (ID of 7 cm). Argon gas was passed for 2 h before increasing temperature and continued throughout the run (1 litre/min). Temperature was increased (to 1200–1550°C) at 4°C/min heating rate followed by 2 h soaking period. The sample was cooled at 4°C/min cooling rate down to 700–800°C where the furnace power was off. The temperature reading was based on a B-type thermocouple located between the alumina tube and molybdenum disilicide heating element.

The lattice parameter, oxygen content, and morphology of the TiC product were studied using XRD, chemical analysis, and transmission electron microscopy (TEM) (Model H7 I OOFA, Hitachi Inc., Tokyo, Japan). Oxygen was analysed by infrared detection in an induction furnace using LECO R0416DR oxygen determinator (LECO, St. Joseph, MI). The lattice parameter of the TiC reaction product was determined by X-ray powder diffractometry with Cu-K_α radiation based upon the extrapolation method.[10]

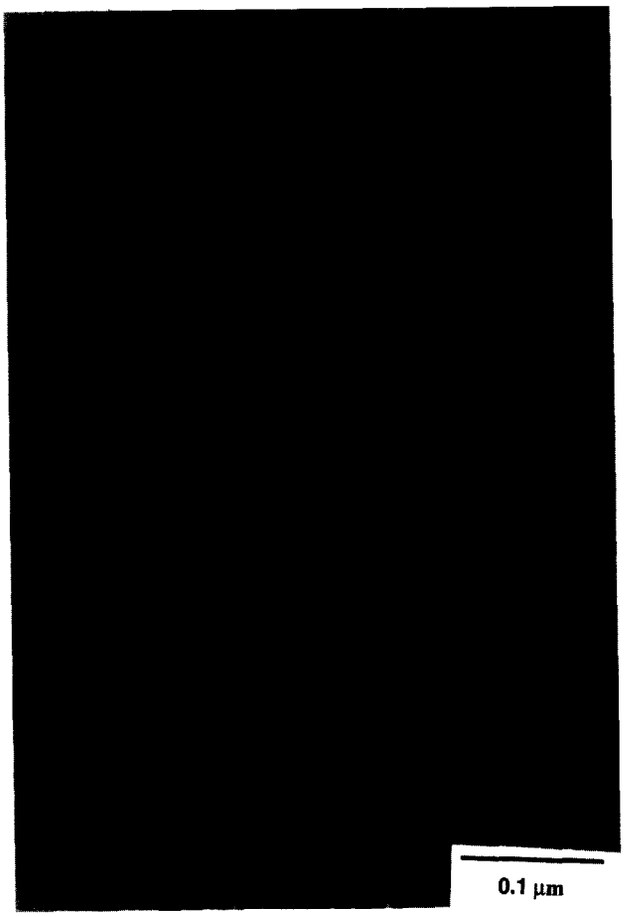

Fig. 2. TEM micrograph of carbon-coated titania precursor.

3 Results and Discussion

3.1 Characterization of carbon-coated titania precursor

Figure 2 shows a bright field TEM micrograph of the carbon-coated titania precursor. As shown in the figure, a very uniform circumferential carbon coating (bright area due to low atomic weight of carbon) on titania particle surfaces is apparent. This shows the effectiveness of the carbon-coating process (on titania surfaces) by the pyrolysis of C_3H_6 gas. The XRD pattern of the carbon-coated titania precursor is shown in Fig. 3 (bottom trace). In the figure, the absence of crystalline carbon phases implies that the deposited carbon in Fig. 1 has amorphous (pyrolytic) structure.

Figure 4 shows the TGA trace (heated at 4°C/min in argon) for the carbon-coated titania precursor (32·6 wt% carbon). For comparison, the result for a carbon black (Monarch 880, Cabot, Waltham, MA)/titania powder mixture with the same carbon content is also shown. In the light of reaction (1), the weight loss of the system indicates the degree of reaction progressed. In Fig. 4, the significant weight loss of the carbon/titania mixture started at about 1100°C while the carbon-coated titania precursor showed similar weight loss at about 900°C. The difference in weight loss

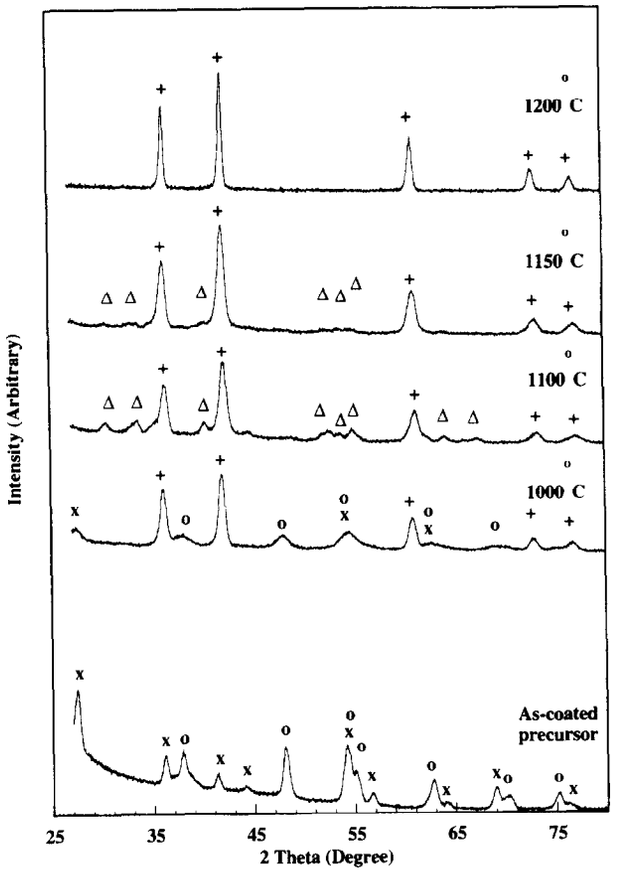

Fig. 3. XRD results of reaction products from carbon-coated titania samples passed through TGA analysis (heat treatment for 2 h at various temperatures). (o): anatase, (x): rutile, (△): Ti_3O_5, and (+): TiC_xO_y.

behavior demonstrates the higher reactivity of the carbon-coated titania precursor as compared to the conventional carbon/titania mixture.

3.2 Phase evolution

XRD patterns from samples passed through the isothermal TGA analysis at various temperatures are shown in Fig. 3. At 1000°C, the system consists of rutile, anatase, and TiC_xO_y phases (as will be shown later using oxygen content and lattice parameter in Fig. 7, initial formation is not pure TiC; it is in fact a solid solution of TiC and TiO with the virtual formula of TiC_xO_y). At 1100°C, a Ti_3O_5 phase appears with increased TiC_xO_y peak intensities. At 1150°C, a trace amount of Ti_3O_5 is identified with further grown TiC_xO_y. Above 1200°C, only TiC_xO_y phase is formed with no other phases.

At 1100°C, the remaining TiO_2 lowers its oxidation states to Ti_3O_5 (monoclinic, JCPDS card number 40-0806). The trace amount of Ti_3O_5 with increased TiC_xO_y at 1150°C indicates the growth of TiC_xO_y at the expense of Ti_3O_5. The TiC_xO_y formation by the latter mechanism is named as the second-stage formation of TiC_xO_y in this work.

The growth of TiC_xO_y from Ti_3O_5 implies that Ti_3O_5 is the lowest oxide phase before forming TiC_xO_y in the second stage. This is inconsistent with other work reporting Ti_2O_3[5,8] or TiO[11] as the lowest oxide of the system while consistent with the observation of Ouensanga[12] who observed Ti_3O_5 from the carbon–titania mixture compressed under a pressure of about 8 ton/cm^2. The presence of TiO was not detected by XRD while its presence was concluded by chemical calculation.[11] Comparing the result of this work with that of Berger[5] and Koc[8] who observed Ti_2O_3 as the lowest oxide before forming TiC_xO_y, the titania source with higher reactivity (such as the precursor used in this work) would be capable of forming TiC_xO_y before it fully lowers its oxidation state to Ti_2O_3.

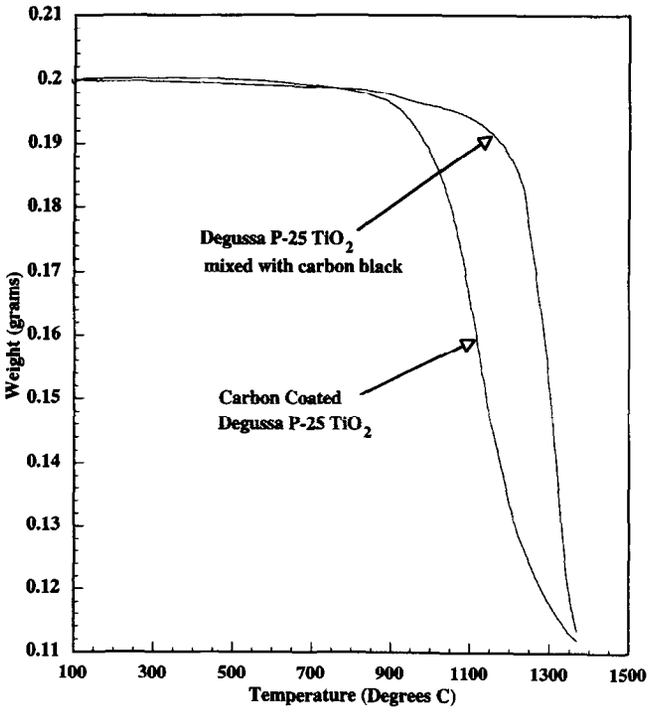

Fig. 4. TGA traces of carbon-coated titania precursor and carbon/titania mixture, heated at 4°C/min.

3.3 Isothermal TGA results

Figure 5 shows the isothermal TGA traces at various temperatures. The fraction of conversion, α, is based on the relation,

$$\alpha = \text{wt\% loss/theoretical wt\% loss}$$

where the theoretical loss limit is 48·33 wt% based on reaction (1). In the figure, the higher the soaking temperature, the more fraction of reaction occurs before reaching the firing temperature, resulting in the higher initial α values.

In Fig. 5, a roughly linear α–time relationship is observed in a range between ~0·58 and ~0·75 (marked as stage II). Based upon this observation, three stages are categorized in the figure (stages I through III). Combining with XRD results, the 1000°C-TGA trace shows that the formation of TiC_xO_y from the intermediate phases is accompanied by considerable weight loss. In the

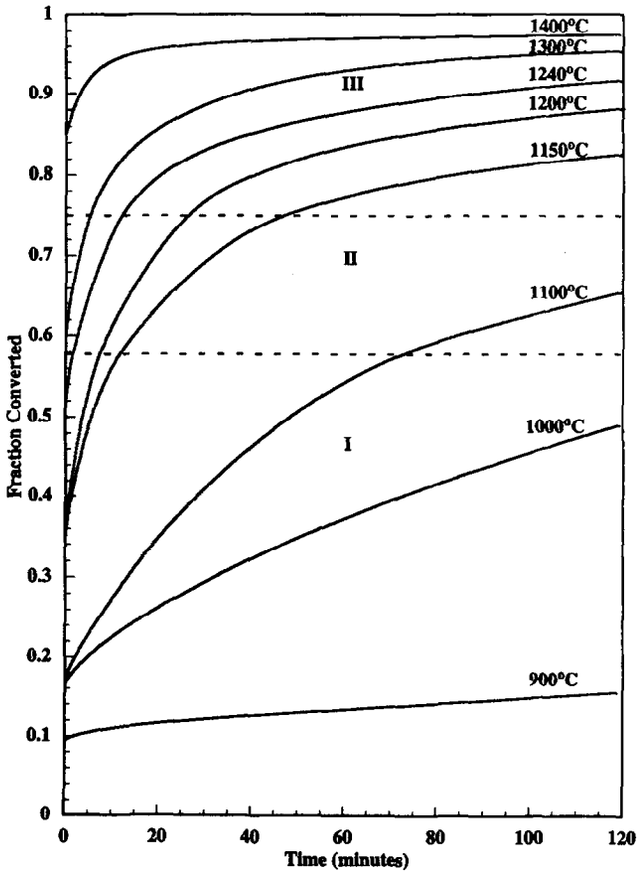

Fig. 5. Isothermal TGA traces at various temperatures.

1100°C-TGA trace, the first stage TiC_xO_y formation would continue until the point where apparent change in trend is observed, implying the start of a different reaction mechanism (stage II).

Considering the observation of Ti_3O_5 after the 1100°C-TGA trace, the linear α–time relationship appearing after an α value of ~0·58 in the TGA trace would be associated with TiO_2 reduction process. After the 1100°C-TGA trace, no appreciable TiO_2 phases are observed, implying that the conversion to Ti_3O_5 is completed. Further weight loss of stage II via the 1150°C-TGA trace showed trace amount of Ti_3O_5 with enhanced TiC_xO_y peak intensities. This indicates that stage II is also associated with the conversion of Ti_3O_5 to TiC_xO_y while no significant change in reaction rate is noticed. The weight loss during stage III would mainly be associated with the purification of the TiC_xO_y phase since no other phases are observed from 1200°C and above.

3.4 Reaction mechanism and activation energy

The first-stage formation of the TiC_xO_y phase (stage I) results in an α value of ~0·55 while the second stage TiC_xO_y formation (stage II) results in an α value of ~0·18. This indicates that the first-stage formation is the major formation process.

The best description of stage II using a linear α–time relation implies that this process may be a reaction-rate-controlled process. Such a linear relation was also observed during the carbothermal reduction of silica[13] where a gas phase (SiO) assisted reaction was recognized. While stage II is basically a reduction process, the solid state diffusion of reducing agent carbon would not result in such a linear relation. The reducing ability of carbon monoxide via equilibrium of CO_2 gas would be a plausible mechanism for such a linear relation:

$$3\ TiO_2(s) + CO(g) = Ti_3O_5(s) + CO_2(g) \quad (4)$$

and

$$Ti_3O_5(s) + 8\ CO(g) = 3\ TiC_xO_y(s) + 5\ CO_2(g) \quad (5)$$

where the equilibrium CO_2/CO ratio is also maintained via reaction

$$CO_2(g) + C(s) = 2\ CO(g) \quad (6)$$

In reaction (5), reaction coefficients are balanced for the case where $x = 1$ and $y = 0$. If the CO_2/CO ratio is governed by reaction (6), TiO_2 and Ti_3O_5 reduction by CO gas is thermodynamically favorable (the Gibbs free energy change of reactions (4)–(6) is the same as their overall reaction, reaction (1)).

The decay of the reaction rate from stage III as compared to stage II may imply the change of reaction mechanism from a reaction-controlled process (stage II) to a diffusion-controlled one (stage III), or reflect decreasing total surface area of Ti_3O_5 as the content of Ti_3O_5 is depleted. The latter reason appeals in this work since a trace amount of Ti_3O_5 is still observed after passing through the 1150°C-TGA trace. A similar change of reaction rate was also observed in the synthesis of SiC[13] where no significant purification of SiC is noticed. Hence it is hard to correlate the trend (shape) of weight loss occurring at the final stage of total reaction (stage III) with the mechanism of TiC_xO_y purification (the purification starts from stage II). Further work is required to uncover the detailed purification mechanism of TiC_xO_y

While the unavailability of initial stage isothermal data of stage I hindered calculation of the reaction rate constant of the diffusion-controlled process, the linear slope of stage II allowed to obtain reaction rate constant k and the result is plotted in terms of ln k versus $1/T$ in Fig. 6. The slope in the figure corresponds to in Arrhenius relation,

$$k = A \exp(-\Delta E/RT)$$

where ΔE is activation energy, A is pre-exponential constant, and RT has its usual meaning. The activation energy of stage II is calculated to be 278·1 kJ/mole.

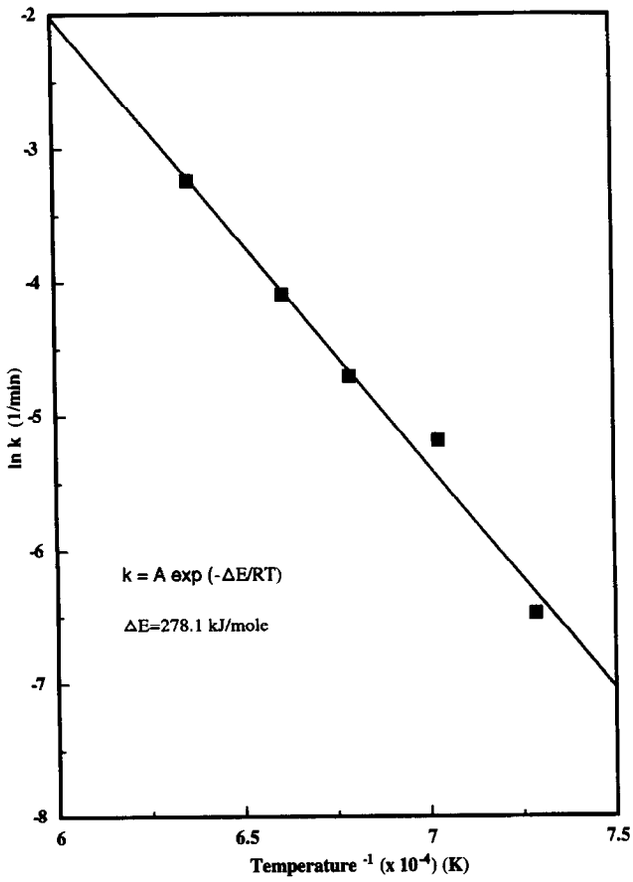

Fig. 6. Arrhenius plot for stage II in Fig. 5.

3.5 Properties of TiC product powder

Figure 7 shows the change in oxygen content and lattice parameter of the TiC product (prepared using a horizontally positioned alumina tube) as a function of production temperature. As can be seen in the figure, the lattice parameter increases with reaction temperature while oxygen content decreases. Since oxygen and nitrogen are common impurities in TiC and are known to lower the lattice parameter of TiC,[14] the observed low lattice parameters of the reaction products with high oxygen content (at 1300–1400°C) could be due to the fact that TiC (a_o = 4·331 Å[6] or 4·328 Å[14]) formed a solid solution with TiO (a_o = 4·180 Å[14]). Figure 7 implies that TiC_xO_y (instead of pure TiC) forms at lower temperature and then it is purified toward TiC at higher temperature.

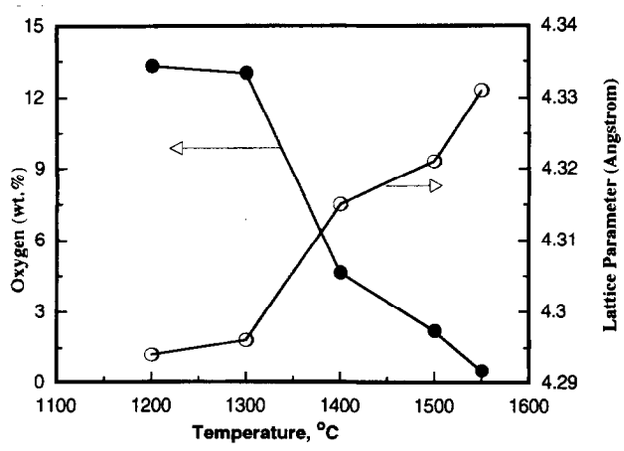

Fig. 7. Change in oxygen content and lattice parameter of TiC powder product as a function of production temperature. Two hours of reaction period at each temperature except for data at 1500°C where 4 h soaking time was allowed.

Fig. 8. TEM micrograph of TiC powder product synthesized at 1500°C for 4 h in flowing argon atmosphere.

The morphology of the TiC product fired at 1550°C for 2 h is shown in Fig. 8 (bright field image of TEM). As shown in the figure, the TiC powders produced have fine particle size (BET surface area with free carbon 21 m^2/g), narrow particle size distribution (0·1–0·3 μm from TEM), and are loosely agglomerated.

4 Conclusion

The carbothermal synthesis of titanium carbide in the present work proceeded via forming titanium oxycarbide followed by the purification of titanium oxycarbide toward pure titanium carbide. The formation of titanium oxycarbide proceeded by two routes. The uniformly coated pyrolytic carbon on fine titania particles formed a TiC_xO_y phase. Then an additional titanium oxycarbide started to form from the Ti_3O_5 phase. Ti_3O_5 was the oxide phase with lowest oxidation state before forming the oxycarbide phase in the additional formation of titanium oxycarbide and the activation energy of the process was 278·1 kJ/mole. The resultant titanium carbide powders prepared at 1550°C for 4 h in flowing argon showed fine particle size (0·1–0·3 μm), oxygen content of 0·57 wt%, lattice parameter of 4·331 Å, uniform particle shape, and loose agglomeration between particles.

Acknowledgment

The author thanks Dr Charles Sorrell for his continued support and interest in this work. The author also wishes to thank Jeffrey S. Folmer for TEM studies. This research was sponsored by the US Department of Energy, Office of Industrial Technologies, as part of the Advanced Industrial Materials Program, under contract DE-AC05-84OR21400 with Lockheed Martin Energy Systems, Inc.

References

1. Andrievskii, R. A., Alekseev, S. A., Dzodziev, G. T., Dzneladze, A. Zh., Travushkin, G. C., Turehin, V. N. and Chertovich, A. F., Physicomechanical properties of titanium carbide with titanium nitride additions. *Soviet Powder Metallurgy and Metal Ceramics*, 1980, **19**(9), 612–615.
2. Halverson, D. C., Ewald, K. H. and Munir, Z. A., Influence of reactant characteristics on the microstructures of

combustion synthesized titanium carbide. *J. Mater. Sci.*, 1993, **28**, 4583–4594.
3. Mihailescu, I. N., De Giorge, M. L., Boulmer-Leborgne, C. H. and Udrea, S., Direct carbide synthesis by multi-pulse exciter laser treatment of Ti samples in ambient CH_4 gas at superatmospheric pressure. *J. Appl. Phys.*, 1994, **75**, 5286–5294.
4. Harbuck, D. D., Davidson, C. F. and Monte, B., Gas phase production of TiN and TiC powders. *J. Metals.*, 1986, **38**, 47–50.
5. Berger, L. M., Titanium carbide synthesis from titanium dioxide and carbon black. *J. Hard Mater.*, 1992, **3**(1), 3–15.
6. Divakar, R., Chia, K. Y., Kunz, S. M. and Lau, S. K., Carbides. In *Encyclopedia of Chemical Technology*, Vol. 4, ed. J. I. Kroschwitz and M. Howe-Grant. J. Wiley and Sons, New York, NY, 1992, pp. 841–911.
7. Tristant, P., Aubreton, J. and Lefort, P., Approche thermodynamique de la reduction carbothermique du dioxyde de titane. *High Temp. Chem. Processes*, 1994, **3**, 375–388.
8. Koc, R., Kinetics and phase evolution during carbothermal synthesis of titanium carbide from ultrafine titania/carbon powder mixture, *J. Mater. Sci.* (submitted).
9. Koc, R. and Glatzmaier, G., Process for synthesizing titanium carbide, titanium nitride and carbonitride, US Patent No. 5,417,952, 1995.
10. Cullity, B. D., *Elements of X-ray Diffraction, 2nd edn.* Addison-Wesley Publishing Company, Inc., Reading, Massachusetts, 1978, 360 pp.
11. Lyubimov, V. D., Alyamovskii, S. I. and Shveikin, G. P., Mechanism of the reduction of titanium oxides by carbon. *Russian J. Inorg. Chem.*, 1981, **26**(9), 1243–1247.
12. Ouensanga, A., Thermodynamic study of the Ti–C–O system in the temperature range 1400–1600 K. *J. Less-Common Met.*, 1979, **63**, 225–235.
13. Lee, J. G. and Cutler, I. B., Formation of silicon carbide from rice hulls. *Am. Ceram. Soc. Bull.*, 1975, **54**(2), 195–198.
14. Storms, E. K., *The Refractory Carbides.* Refractory Materials Series, Vol. 2, Academic Press, New York, 1967.